

LEFORMER: A HYBRID CNN-TRANSFORMER ARCHITECTURE FOR ACCURATE LAKE EXTRACTION FROM REMOTE SENSING IMAGERY

Ben Chen^{1,*}, Xuechao Zou^{1,*}, Yu Zhang¹, Jiayu Li¹, Kai Li², Junliang Xing², Pin Tao^{1,2†}

¹Qinghai University, Department of Computer Technology and Applications, Xining, China

²Tsinghua University, Department of Computer Science and Technology, Beijing, China

ABSTRACT

Lake extraction from remote sensing images is challenging due to the complex lake shapes and inherent data noises. Existing methods suffer from blurred segmentation boundaries and poor foreground modeling. This paper proposes a hybrid CNN-Transformer architecture, called LEFormer, for accurate lake extraction. LEFormer contains three main modules: CNN encoder, Transformer encoder, and cross-encoder fusion. The CNN encoder effectively recovers local spatial information and improves fine-scale details. Simultaneously, the Transformer encoder captures long-range dependencies between sequences of any length, allowing them to obtain global features and context information. The cross-encoder fusion module integrates the local and global features to improve mask prediction. Experimental results show that LEFormer consistently achieves state-of-the-art performance and efficiency on the Surface Water and the Qinghai-Tibet Plateau Lake datasets. Specifically, LEFormer achieves 90.86% and 97.42% mIoU on two datasets with a parameter count of 3.61M, respectively, while being 20× minor than the previous best lake extraction method. The source code is available at <https://github.com/BastianChen/LEFormer>.

Index Terms— Lake Extraction, CNN, Transformer, Segmentation

1. INTRODUCTION

Lakes are crucial environmental and climatic indices that have gained focus [1]. Advancements in worldwide observation technologies and sensing equipment have made remote sensing images a common means for extracting hydrological features [2]. Automated extraction of lakes from remote sensing data is critical to track climate alterations [3].

Lake extraction has generally been considered a semantic segmentation task. Recently, researchers have utilized deep learning methods for lake extraction, such as UDGNet [4], to boost the spatial resolution of lake zones. MSLWENet [5] proposes an end-to-end multi-scale plateau lake extraction network model based on ResNet-101 [6] and depth-wise separable

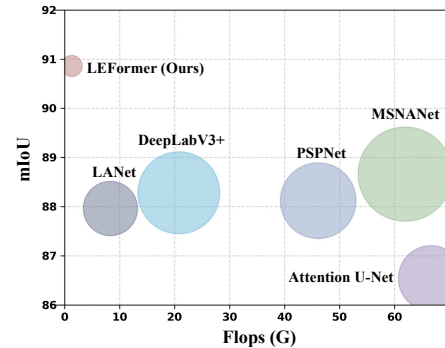


Fig. 1. Performance and efficiency comparison on Surface Water dataset. The circle area indicates the number of parameters.

convolution [7]. HA-Net [2] presents a mixed-scale attention mechanism, while MSNANet [8] employs an encoder-decoder backbone to improve feature representation and achieve superior lake extraction outcomes. Nevertheless, the extraction of lakes remains challenging due to high interclass heterogeneity and complex background information, such as snow, glaciers, and mountains, which introduce contextual ambiguity and pose additional extraction challenges.

To address the limitations of existing models, we propose an efficient architecture (LEFormer) for extracting lakes from remote sensing imagery by combining CNN and Transformer architectures. Our architecture leverages CNN to extract local features and Transformer to capture global features. The cross-encoder fusion module fuses the local and global features extracted by the CNN and Transformer into a unified feature used as input to the generated lake mask. These modules achieve high accuracy and low computational cost with a lightweight network structure, as shown in Fig. 1. The main contributions of our architecture are summarized as follows:

- We introduce LEFormer, a novel architecture for lake extraction. LEFormer combines CNN and Transformer to capture local and global features and employs cross-encoder fusion modules to improve mask prediction.
- We design a CNN encoder with multi-scale spatial-channel attention (MSCA) to extract precise and detailed

*These authors contributed equally.

†Corresponding author.

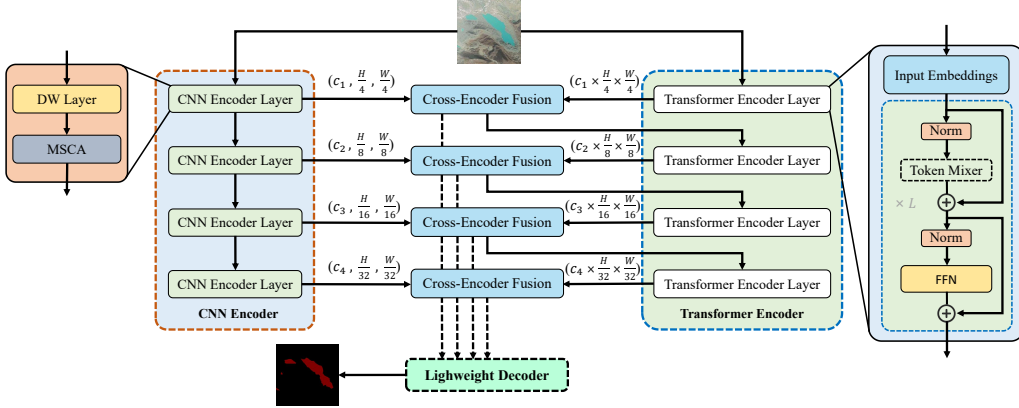


Fig. 2. Overview architecture of our proposed LEFormer.

local spatial information.

- We develop a lightweight Transformer encoder, reducing the computational and parameter demands of the model while maintaining high performance.

2. METHODOLOGY

In this study, we propose the LEFormer, a novel architecture for high-performance lake extraction. Illustrated in Fig. 2, LEFormer contains three main modules: (1) CNN Encoder (CE) for precise local spatial information extraction; (2) Transformer Encoder (TE) for capturing long-range dependencies and global context; (3) lightweight Cross-Encoder Fusion (CEF) module for integrating features from TE and CE.

2.1. CNN Encoder (CE)

Our proposed CE is based on a hierarchical structure consisting of multiple stacked CE layers. Each CE Layer comprises a depth-wise separable (DW) layer [7] and an MSCA, facilitating improved multi-scale feature extraction. We use the DW Layer as down-sampling stages to down-sample the input image to sizes of $\frac{H}{4} \times \frac{W}{4}$, $\frac{H}{8} \times \frac{W}{8}$, $\frac{H}{16} \times \frac{W}{16}$, and $\frac{H}{32} \times \frac{W}{32}$, where H and W denote the height and width of the input image. Each down-sampling stage contains a down-sampling block with a convolutional layer (detailed settings are listed in Table 1) and a GELU activation function [9].

In addition, we integrate an MSCA that combines the benefits of dilated convolutions [10] and CBAM [11] for enhanced multi-scale feature extraction. Dilated convolutions can improve segmenting objects or features of different scales by adjusting the kernel dilation rate. We first utilize dilated convolutions with 1, 2, 3, and 4 dilation rates to generate multi-scale feature maps. Next, we apply the CBAM layer to compute attention weighting for the extracted multi-scale feature maps and multiply it with the input multi-scale feature maps to obtain the final features. The CBAM layer employs channel

Table 1. The detailed settings of our LEFormer, including patch size (K_i), stride (S_i), padding size (P_i), channel number (C_i), reduction ratio (R_i), head number (N_i) and number of encoder blocks (L_i) in Stage i .

Stage	Output Size	CNN Encoder	Transformer Encoder
1	$\frac{H}{4} \times \frac{W}{4}$	$K_1 = 7; S_1 = 4;$ $P_1 = 3; C_1 = 32$	$R_1 = 8; N_1 = 1; L_1 = 2$
2	$\frac{H}{8} \times \frac{W}{8}$	$K_2 = 3; S_2 = 2;$ $P_2 = 1; C_2 = 64$	$R_2 = 4; N_2 = 2; L_2 = 2$
3	$\frac{H}{16} \times \frac{W}{16}$	$K_3 = 3; S_3 = 2;$ $P_3 = 1; C_3 = 160$	$R_3 = 2; N_3 = 5; L_3 = 2$
4	$\frac{H}{32} \times \frac{W}{32}$	$K_4 = 3; S_4 = 2;$ $P_4 = 1; C_4 = 192$	$R_4 = 1; N_4 = 6; L_4 = 3$

and spatial attention mechanisms that dynamically allocate weights to the features of the captured lake mask, effectively enhancing the model’s feature representation and discrimination capability. This combination of techniques enables efficient aggregation of relevant information at multiple scales while minimizing computational cost. The structure of the MSCA is illustrated in Fig. 3.

2.2. Transformer Encoder (TE)

Motivated by Transformers’ success in computer vision, we propose a lightweight TE layer. ViT [12] lacks local continuity among patches and requires positional embedding interpolation when test resolution differs from training, reducing accuracy. To address this, we adopt Overlapped Patch Merging from SegFormer [13], with the same configuration as CE.

FFN uses a 2D convolutional layer with a kernel size of 3×3 to extract positional information instead of traditional positional encoding, expressed as follows:

$$\mathbf{F}_{out} = \text{MLP}(\text{GELU}(\text{Conv}_{3 \times 3}(\text{MLP}(\mathbf{F}_{in})))) + \mathbf{F}_{in}. \quad (1)$$

In addition to the above issues, the self-attention process is computationally expensive and has a complexity of $\mathcal{O}(N^2)$,

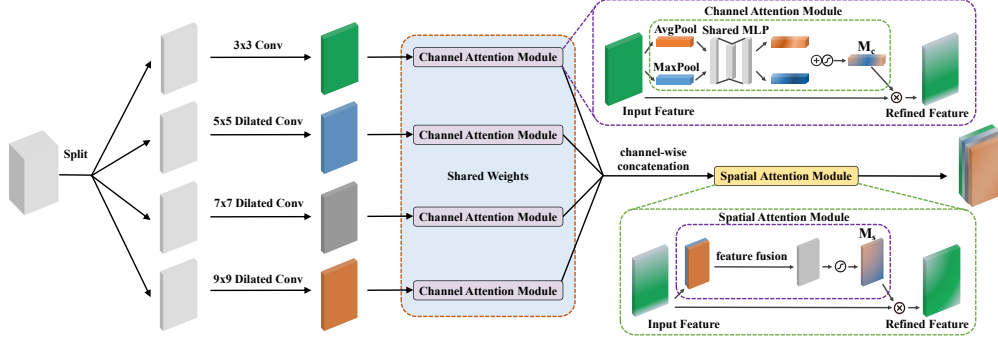


Fig. 3. The diagram depicts the structural layout of the MSCA.

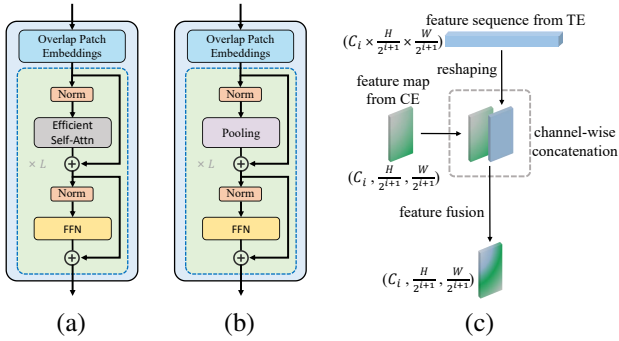


Fig. 4. The diagram depicts the structural layout of three critical modules: (a) the Efficient Transformer Layer (ETL), (b) the Pooling Transformer Layer (PTL), and (c) the Cross-Encoder Fusion (CEF).

making it impractical for large image resolutions. Efficient Self-Attention [13] tackles this problem by utilizing the sequence reduction process from PVT [14], which reduces the sequence length using a reduction ratio R as follows:

$$\hat{\mathbf{K}} = \text{CONV}_{R \times R}(\text{Reshape}(C, H, W))(\mathbf{K})$$

$$\mathbf{K} = \text{Reshape}\left(\frac{N}{R^2}, C\right)(\hat{\mathbf{K}}), \quad (2)$$

where N denotes $H \times W$. Efficient Self-Attention reduces sequence \mathbf{K} using a $\text{CONV}_{R \times R}$ layer and $\text{Reshape}\left(\frac{N}{R^2}, C\right)(\hat{\mathbf{K}})$. It reshapes \mathbf{K} into a (C, H, W) tensor, applies $\text{CONV}_{R \times R}$ to generate $(C, \frac{H}{R}, \frac{W}{R})$, and uses $\text{Reshape}\left(\frac{N}{R^2}, C\right)$ to reduce $\hat{\mathbf{K}}$ to $\frac{N}{R^2} \times C$. This reduces self-attention complexity from $\mathcal{O}(N^2)$ to $\mathcal{O}\left(\frac{N^2}{R^2}\right)$. Overlapped Patch Merging, FFN, and Efficient Self-Attention form an ETL (Fig. 4(a)). Inspired by PoolFormer’s [15] success in the lightweight vision transformer domain, we combine Overlapped Patch Merging, FFN, and a spatial pooling operator to form a PTL (Fig. 4(b)). This work combines ETL and PTL by designing four Encoder Layers. The first layer employs PTL, while the subsequent three layers employ ETL to extract global features while minimizing computational cost. Refer to Table 1 for more details.

2.3. Cross-Encoder Fusion (CEF)

We propose a lightweight layer (Fig. 4(c)) that combines local features from the CE Layer with global features from the TE layer. The CE layer’s feature map has size $(C_i, \frac{H}{2^{i+1}}, \frac{W}{2^{i+1}})$, while the TE layer’s feature sequence has size $(C_i \times \frac{H}{2^{i+1}} \times \frac{W}{2^{i+1}})$, where $i \in 1, 2, 3, 4$. To integrate these features, the sequence is reshaped to $(C_i, \frac{H}{2^{i+1}}, \frac{W}{2^{i+1}})$ and concatenated with the feature map. The concatenated features are fused using a pointwise convolution layer. In summary, CEF complements the TE Layer’s output with the CE Layer’s output, recovering local spatial information and enhancing fine-scale details. The output of all CEF layers is passed through a lightweight decoder from SegFormer to predict the final mask.

3. EXPERIMENTS

3.1. Experimental Settings

Datasets. This study evaluates the LEFormer’s performance and generalization capability on two publicly satellite remote sensing datasets for lake extraction: the Surface Water dataset (SW dataset) and the Qinghai-Tibet Plateau Lake dataset (QTPL dataset) [5]. Both datasets include annotated lake water bodies from visible spectrum remote sensing images of size 256×256 . The SW dataset comprises 17,596 images divided by 4:1 for training and testing, while the QTPL dataset contains 6,773 images divided by 9:1 for training and testing. **Implementation details.** The models are trained on a single Tesla V100 GPU using the *MMSegmentation* codebase for 160K iterations on the SW and QTPL datasets. Data augmentation, such as random resizing and horizontal flipping, to enhance generalization. The AdamW [16] optimizer and cross-entropy loss function [17] are used with a batch size of 16. The initial learning rate and weight decay are set to 6×10^{-5} and 0.01, respectively. The learning rate is dynamically adjusted using a PolyScheduler [18] with a factor of 1.0. The models’ accuracy is evaluated using overall accuracy (OA), F1, and mean Intersection over Union (mIoU). The efficiency is assessed by the parameter (Params, M) and

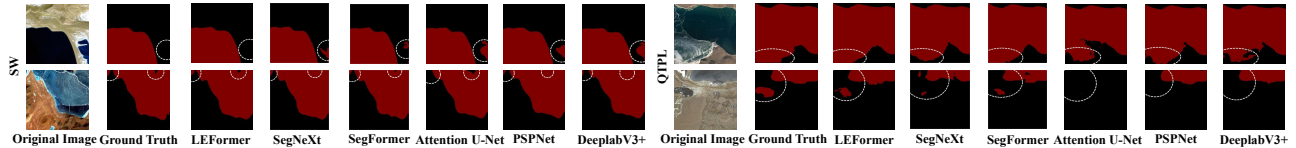


Fig. 5. Visualization results of our proposed LEFormer and other methods. The white circles indicate apparent differences.

Table 2. Impact of the number of PTLs on model parameters, flops, and accuracy (L denotes the number of layers).

L	#P↓	#F↓	SW			QTPL		
			OA↑	F1↑	mIoU↑	OA↑	F1↑	mIoU↑
4	3.24	1.23	94.68	92.35	88.98	98.39	98.03	96.72
3	3.26	1.24	95.04	92.88	89.69	98.64	98.33	97.22
2	3.48	1.25	95.52	93.57	90.64	98.66	98.36	97.26
1	3.61	1.27	95.63	93.73	90.86	98.74	98.45	97.42
0	3.74	1.28	95.62	93.72	90.84	98.71	98.42	97.36

Table 3. Impact of different encoder combinations on #P, #F, and accuracy (ETL + PTL denotes three ETLs and one PTL).

Dataset	CE		TE		#P↓	#F↓	OA↑	F1↑	mIoU↑
	DW	MSCA	ETL	PTL					
SW	×	×	✓	×	3.22	1.09	95.60	93.68	90.79
	×	×	✓	✓	3.09	1.07	95.41	93.40	90.41
	✓	✓	×	×	0.74	0.82	94.32	91.84	88.28
	✓	×	✓	✓	3.46	1.23	95.55	93.60	90.69
	✓	✓	✓	×	3.74	1.28	95.62	93.72	90.84
	✓	✓	✓	✓	3.61	1.27	95.63	93.73	90.86
QTPL	×	×	✓	×	3.22	1.09	98.65	98.35	97.25
	×	×	✓	✓	3.09	1.07	98.62	98.31	97.18
	✓	✓	×	×	0.74	0.82	98.36	97.99	96.66
	✓	×	✓	✓	3.46	1.23	98.64	98.34	97.22
	✓	✓	✓	×	3.74	1.28	98.71	98.42	97.36
	✓	✓	✓	✓	3.61	1.27	98.74	98.45	97.42

floating point operations per second (Flops, G), denoted as #P and #F, respectively, in the table for brevity.

3.2. Ablation Studies

Ablation studies are conducted to evaluate the impact of the number of PTLs on the model’s performance on the SW and QTPL datasets. The results (Table 2) demonstrate that the highest accuracy is achieved with $L = 1$ (one PTL and three ETLs). This suggests that the PTL can be effectively utilized when the model suits the dataset. However, excessive use of the PTL can lead to reduced accuracy.

We also conduct ablation studies to assess different encoder combinations’ impact on performance and efficiency based on Table 3. TE with ETL and PTL achieves 90.41% and 97.18% mIoU on SW and QTPL. In contrast, CE with MSCA achieves 88.28% and 96.66% mIoU, indicating TE effectively captures long-range dependencies and global context. Additionally, including DW improves mIoU by 0.28% and 0.04%. MSCA improves mIoU by 0.17% and 0.20%, suggesting DW and MSCA contribute to accuracy. Omitting CE, PTL reduces

Table 4. Quantitative comparison of our LEFormer and other methods on the SW and QTPL datasets.

Method	#P↓	#F↓	SW / QTPL		
			OA↑	F1↑	mIoU↑
PSPNet [19]	46.80	46.11	94.17 / 98.40	91.73 / 98.03	88.12 / 96.77
DeeplabV3+ [20]	54.70	20.76	94.30 / 98.39	91.87 / 98.03	88.28 / 96.75
Attention U-Net [21]	34.90	66.64	93.34 / 98.24	90.56 / 97.87	86.54 / 96.42
LANet [22]	24.00	8.31	94.14 / 98.29	91.62 / 97.89	87.96 / 96.52
SegFormer [13]	3.72	1.59	95.58 / 98.66	93.65 / 98.36	90.75 / 97.27
SegNeXt [23]	4.26	1.55	95.50 / 98.60	93.56 / 98.30	90.61 / 97.15
MSNANet [8]	72.30	61.94	94.44 / 98.47	92.12 / 98.11	88.66 / 96.88
LEFormer (Ours)	3.61	1.27	95.63 / 98.74	93.73 / 98.45	90.86 / 97.42

mIoU by 0.38% and 0.07%. However, with DW and MSCA, PTL does not decrease metrics and results in a lighter model.

3.3. Comparison to the State-of-the-Arts

We assess the efficacy of LEFormer by comparing it with advanced lake extraction models [8, 23, 13, 22, 21, 20, 19] on the SW and QTPL datasets. Table 4 summarizes the quantitative results and visualization results in Fig. 5.

As shown in Table 4, LEFormer outperforms all other models regarding parameters, flops, and accuracy. On the SW dataset, LEFormer achieves 90.86% mIoU using only 3.61M parameters and 1.27G flops. Compared to the previous lake extraction method MSNANet, LEFormer is 20× minor and requires 48× fewer flops while achieving a 2.20% better mIoU. On the QTPL dataset, LEFormer also achieves SOTA performance. In summary, these results demonstrate the superiority of LEFormer in the lake extraction task.

4. CONCLUSION

In this study, we propose the LEFormer, a hybrid CNN-Transformer architecture for accurate lake extraction. We combine CNNs and Transformers to capture short- and long-range dependencies to obtain robust features for lake mask prediction. Experiments show that LEFormer achieves SOTA performance and efficiency on two benchmark datasets. We hope that LEFormer will encourage the design of efficient hybrid CNN-Transformer networks for lake extraction.

5. ACKNOWLEDGEMENTS

This work is supported in part by the Natural Science Foundation of China under Grant No. 62222606 and 62076238.

6. REFERENCES

- [1] Jieyu Lu, Yubao Qiu, Xingxing Wang, Wenshan Liang, Pengfei Xie, Lijuan Shi, Massimo Menenti, and Dongshui Zhang, “Constructing dataset of classified drainage areas based on surface water-supply patterns in high mountain asia,” *BIG EARTH DATA*, vol. 4, no. 3, pp. 225–241, 2020.
- [2] Zhaobin Wang, Xiong Gao, and Yaonan Zhang, “Ha-net: A lake water body extraction network based on hybrid-scale attention and transfer learning,” *Remote Sensing*, vol. 13, no. 20, pp. 4121, 2021.
- [3] Zhihui Tian, Xiaoyu Guo, Xiaohui He, Panle Li, Xijie Cheng, and Guangsheng Zhou, “Mscanet: multi-scale context information aggregation network for tibetan plateau lake extraction from remote sensing images,” *Int. J. Digit. Earth*, vol. 16, no. 1, pp. 1–30, 2023.
- [4] Mengjiao Qin, Linshu Hu, Zhenhong Du, Yi Gao, Lianjie Qin, Feng Zhang, and Renyi Liu, “Achieving higher resolution lake area from remote sensing images through an unsupervised deep learning super-resolution method,” *Remote Sensing*, vol. 12, no. 12, pp. 1937, 2020.
- [5] Zhaobin Wang, Xiong Gao, Yaonan Zhang, and Guohui Zhao, “Mslwenet: A novel deep learning network for lake water body extraction of google remote sensing images,” *Remote Sensing*, vol. 12, no. 24, pp. 4140, 2020.
- [6] Kaiming He, Xiangyu Zhang, Shaoqing Ren, and Jian Sun, “Deep residual learning for image recognition,” in *CVPR*, 2016, pp. 770–778.
- [7] François Chollet, “Xception: Deep learning with depthwise separable convolutions,” in *CVPR*, 2017, pp. 1251–1258.
- [8] Xin Lyu, Yiwei Fang, Baogen Tong, Xin Li, and Tao Zeng, “Multiscale normalization attention network for water body extraction from remote sensing imagery,” *Remote Sensing*, vol. 14, no. 19, pp. 4983, 2022.
- [9] Dan Hendrycks and Kevin Gimpel, “Bridging nonlinearities and stochastic regularizers with gaussian error linear units,” *arXiv:1606.08415*, 2016.
- [10] Sachin Mehta, Mohammad Rastegari, Anat Caspi, Linda Shapiro, and Hannaneh Hajishirzi, “Espnet: Efficient spatial pyramid of dilated convolutions for semantic segmentation,” in *ECCV*, 2018, pp. 561–580.
- [11] Sanghyun Woo, Jongchan Park, Joon-Young Lee, and In So Kweon, “Cbam: Convolutional block attention module,” in *ECCV*, 2018, pp. 3–19.
- [12] Alexey Dosovitskiy, Lucas Beyer, Alexander Kolesnikov, Dirk Weissenborn, Xiaohua Zhai, Thomas Unterthiner, Mostafa Dehghani, Matthias Minderer, Georg Heigold, Sylvain Gelly, Jakob Uszkoreit, and Neil Houlsby, “An image is worth 16x16 words: Transformers for image recognition at scale,” in *ICLR*, 2021.
- [13] Enze Xie, Wenhai Wang, Zhiding Yu, Anima Anandkumar, Jose M Alvarez, and Ping Luo, “Segformer: Simple and efficient design for semantic segmentation with transformers,” *NeurIPS*, vol. 34, pp. 12077–12090, 2021.
- [14] Wenhai Wang, Enze Xie, Xiang Li, Deng-Ping Fan, Kaitao Song, Ding Liang, Tong Lu, Ping Luo, and Ling Shao, “Pyramid vision transformer: A versatile backbone for dense prediction without convolutions,” in *ICCV*, 2021, pp. 548–558.
- [15] Weihao Yu, Mi Luo, Pan Zhou, Chenyang Si, Yichen Zhou, Xinchao Wang, Jiashi Feng, and Shuicheng Yan, “Metaformer is actually what you need for vision,” in *CVPR*, 2022, pp. 10819–10829.
- [16] Ilya Loshchilov and Frank Hutter, “Decoupled weight decay regularization,” in *ICLR*, 2019.
- [17] David E Rumelhart, Geoffrey E Hinton, and Ronald J Williams, “Learning representations by back-propagating errors,” *Nature*, vol. 323, no. 6088, pp. 533–536, 1986.
- [18] Kaiming He, Georgia Gkioxari, Piotr Dollár, and Ross B. Girshick, “Mask r-cnn,” in *ICCV*, 2017, pp. 2980–2988.
- [19] Hengshuang Zhao, Jianping Shi, Xiaojuan Qi, Xiaogang Wang, and Jiaya Jia, “Pyramid scene parsing network,” in *CVPR*, 2017, pp. 2881–2890.
- [20] Liang-Chieh Chen, Yukun Zhu, George Papandreou, Florian Schroff, and Hartwig Adam, “Encoder-decoder with atrous separable convolution for semantic image segmentation,” in *ECCV*, 2018, pp. 801–818.
- [21] Jo Schlemper, Ozan Oktay, Michiel Schaap, Mattias Heinrich, Bernhard Kainz, Ben Glocker, and Daniel Rueckert, “Attention gated networks: Learning to leverage salient regions in medical images,” *Medical Image Anal.*, vol. 53, pp. 197–207, 2019.
- [22] Lei Ding, Hao Tang, and Lorenzo Bruzzone, “Lanet: Local attention embedding to improve the semantic segmentation of remote sensing images,” *TGRS*, vol. 59, no. 1, pp. 426–435, 2021.
- [23] Meng-Hao Guo, Cheng-Ze Lu, Qibin Hou, Zhengning Liu, Ming-Ming Cheng, and Shi-Min Hu, “Segnext: Rethinking convolutional attention design for semantic segmentation,” *NeurIPS*, vol. 35, pp. 1140–1156, 2022.